




## Relative benefits of allocating land to bioenergy crops and forests vary by region

Irina Melnikova <sup>1,2</sup>✉, Philippe Ciais <sup>1</sup>, Katsumasa Tanaka <sup>1,2</sup>, Nicolas Vuichard<sup>1</sup> & Olivier Boucher<sup>3</sup>

Carbon dioxide removal is essential for achieving the Paris Agreement targets. Here we compare bioenergy with carbon capture and storage (BECCS) and afforestation and reforestation in terms of their carbon removal potentials and impacts on carbon cycle and surface climate under an overshoot pathway using Earth System Model simulations. Although initially BECCS can remove more carbon in allocated areas, carbon dioxide emissions from land use change regionally offset the benefits of BECCS compared to afforestation, depending on the carbon capture and storage efficiency and timescales required to achieve mitigation targets. Furthermore, BECCS may cause local cooling in high- and mid-latitude subregions of the Northern Hemisphere dominated by albedo effects, while afforestation causes local cooling in subtropical and tropical subregions through non-radiative mechanisms. The decision to allocate land to bioenergy crops or forests should account for their respective carbon removal potentials, modulated by carbon-concentration and carbon-climate feedbacks, and the effects on climate.

<sup>1</sup>Laboratoire des Sciences du Climat et de l'Environnement (LSCCE), Institut Pierre-Simon Laplace (IPSL), CEA/ CNRS/ UVSQ, Université Paris-Saclay, Gif-sur-Yvette, France. <sup>2</sup>Earth System Division, National Institute for Environmental Studies (NIES), Tsukuba, Japan. <sup>3</sup>IPSL, Sorbonne Université / CNRS, Paris, France. ✉email: [melnikova.irina@nies.go.jp](mailto:melnikova.irina@nies.go.jp)

Negative emissions that rely on carbon dioxide removal (CDR) are projected to play an important role in achieving the net zero greenhouse gas (GHG) emissions and temperature targets of the Paris Agreement, provided they are accompanied by a simultaneous rapid and substantial reduction of GHG emissions<sup>1</sup>. Among existing and putative CDR methods, bioenergy with carbon capture and storage (BECCS) is one of the most cost-effective options in future mitigation pathways<sup>2–4</sup>. BECCS relies on crops to capture carbon through biomass growth and stores the resulting CO<sub>2</sub> after combustion in geological reservoirs for thousands of years<sup>5</sup>. Among the bioenergy dedicated crops, second-generation (2G) crops are particularly promising because they do not directly compete with crops for food production and may increase the soil organic carbon content to some extent when cultivated in low-carbon-content lands<sup>4,6,7</sup>. Integrated assessment models (IAMs) show that a large-scale deployment of 2G bioenergy crops can be a key component to achieving the net-zero GHG emission target by the end of the 21<sup>st</sup> century<sup>8–10</sup>. However, challenges related to large-scale bioenergy crop deployment remain. They include large fertilizer applications and water demand, risks to environmental sustainability, and various socio-economic concerns, such as impacts on ecosystem services, social acceptability, local land rights, the capacity of infrastructure, and logistics<sup>2,7,11</sup>. The benefits of BECCS are also partly offset by land-use change (LUC) emissions and are limited by techno-economic developments and regional carbon storage capacities<sup>3,4,12–14</sup>. Besides, BECCS is still at an early stage of development and has not been commercially established or proven at a sufficient scale<sup>15,16</sup>.

Another widely-used and well-developed CDR method is afforestation and reforestation (AR). It currently removes  $0.5 \pm 0.2$  GtC year<sup>-1</sup> from the atmosphere<sup>12,16,17</sup>. AR provides co-benefits for human well-being and receives broad societal support<sup>18</sup>. However, unlike BECCS, which can fix carbon in the geological reservoirs nearly permanently, AR stores carbon in plant biomass and soils only on the timescales of several decades to centuries (non-permanently), and the storage saturates over time. Furthermore, AR is also subject to natural and anthropogenic disturbances, such as fires, pests, degradation, and deforestation<sup>3,16,18–20</sup>.

BECCS and AR are the two most widely-used land-based CDR methods in future mitigation pathways developed by IAMs. They are contrasted in nature as they can be seen as engineered and natural CDR methods, respectively. Both are critically dependent on land availability, which may limit their potential<sup>3</sup>. Combining these CDR methods may be more beneficial because it may reduce deployment failures and storage limitations<sup>3,21–23</sup>. There has been a growing body of studies on the benefits and tradeoffs of different CDR methods<sup>3,12,24,25</sup>. However, these studies are predominantly based on IAMs that have only a simple or limited representation of Earth System processes with low sectoral and geographical details and thus cannot fully account for carbon-climate feedbacks on the carbon removal by BECCS and AR<sup>3,12,22,26,27</sup>. Several studies based on the intermediate complexity models or Earth System Models (ESM) with a more spatially-resolved and detailed representation of processes compare the land-based CDR methods in terms of their potentials for carbon removal and interactions with the Earth System processes<sup>21,22,28,29</sup>. A study investigating the biogeochemical (carbon cycle) feedbacks of land-based mitigation options showed that AR is more beneficial than BECCS in areas of high vegetation and soil carbon contents due to avoided LUC emissions<sup>29</sup>. Another study that looked at both biogeochemical and biogeophysical (climate) effects of bioenergy crop deployment showed that in some regions, biogeophysical warming effects could offset the biogeochemical cooling effects of BECCS through carbon

removal<sup>14</sup>. There is a need to explore the carbon removal of land-based methods and their interactions with global and regional Earth System processes under socially-relevant mitigation pathways.

In this study, we compare the potentials for carbon removal by BECCS and AR and their impacts on the global and regional land carbon cycle and climate system by using an ESM accounting for biogeochemical and biogeophysical feedbacks. We define the carbon removal as a net CO<sub>2</sub> flux including LUC emissions that can be removed from the vegetation and soil carbon pools at a given time without considering any limitation in geological storage due to logistics and/or its capacity. We use the Shared Socioeconomic Pathway (SSP) overshoot scenario SSP5-3.4-OS, which incorporates the 2G bioenergy-crop deployment with CCS<sup>4,9</sup> and has spatially explicit land use maps for planting 2G crops and/or forests (see Fig. 1). To supplement the existing SSP5-3.4-OS simulations using the state-of-the-art ESM IPSL-CM6A-LR, we perform additional simulations assuming large-scale afforestation instead of bioenergy crop deployment based on the land-use maps of SSP5-3.4-OS. By comparing the impacts of BECCS and AR on the land carbon cycle and surface climate, we strive to clarify the optimal regional allocation of bioenergy crops and forests to increase their carbon removal and climate mitigation effects under future mitigation strategies.

Our results suggest that the carbon removal of BECCS exceeds that of AR on a global scale for the same allocated areas (see Supplementary Table S1). However, it varies within regions (across target areas of bioenergy crops or forest allocation, hereafter referred to as subregionally) and over time and depends on the permanently captured carbon fraction of bioenergy crops' yield. Carbon removal benefits are compromised by regionally contrasting impacts on climate due to differences in surface properties between bioenergy crops and forests (such as albedo, roughness, surface humidity, extreme heats) and on the carbon cycle (including the CO<sub>2</sub> fertilization effect and the impacts of changes in temperature, humidity, etc. on carbon sequestration). Since the choice of the land-based CDR method can influence the carbon cycle and climate, which can further influence the carbon removal, a decision to allocate a land area to bioenergy crops or forests should account for potentials for carbon removal, and the effects of biogeophysical and biogeochemical feedbacks.

## Results and discussion

**Biogeophysical feedbacks.** The choice of the CDR method impacts climate globally and regionally through the biogeophysical effects of land cover change<sup>30–32</sup>. The biogeophysical effects are dominated by changes in the surface energy fluxes and contain radiative changes (related to the shortwave and longwave radiative fluxes at surface) and non-radiative mechanisms (related to the sensible, latent, and ground surface heat fluxes). The spatial patterns of biogeophysical effects of BECCS and AR experiments are largely consistent with existing studies<sup>31</sup>, but we extend the scope to the context of bioenergy crops, as well as AR, on the low carbon-content ecosystems.

The standard (with BECCS) concentration-driven SSP5-3.4-OS simulation by IPSL-CM6A-LR gives a maximum global surface air temperature (GSAT) increase of 3.4°C in 2064 and a subsequent decrease to +3.0°C in 2090–2100 relative to a baseline of 1850–1899 (Fig. 1). The GSAT increase is dominated by the radiative effect of increasing CO<sub>2</sub> concentration. It is complemented by the radiative effect of non-CO<sub>2</sub> forcers and CO<sub>2</sub> physiological warming, e.g., warming due to the effect of altered CO<sub>2</sub> on plant physiology (e.g., stomatal closure), which may account for 11–16% of combined CO<sub>2</sub> warming<sup>33</sup>. The non-CO<sub>2</sub> GHGs and CO<sub>2</sub> physiological warming peaks in 2055,

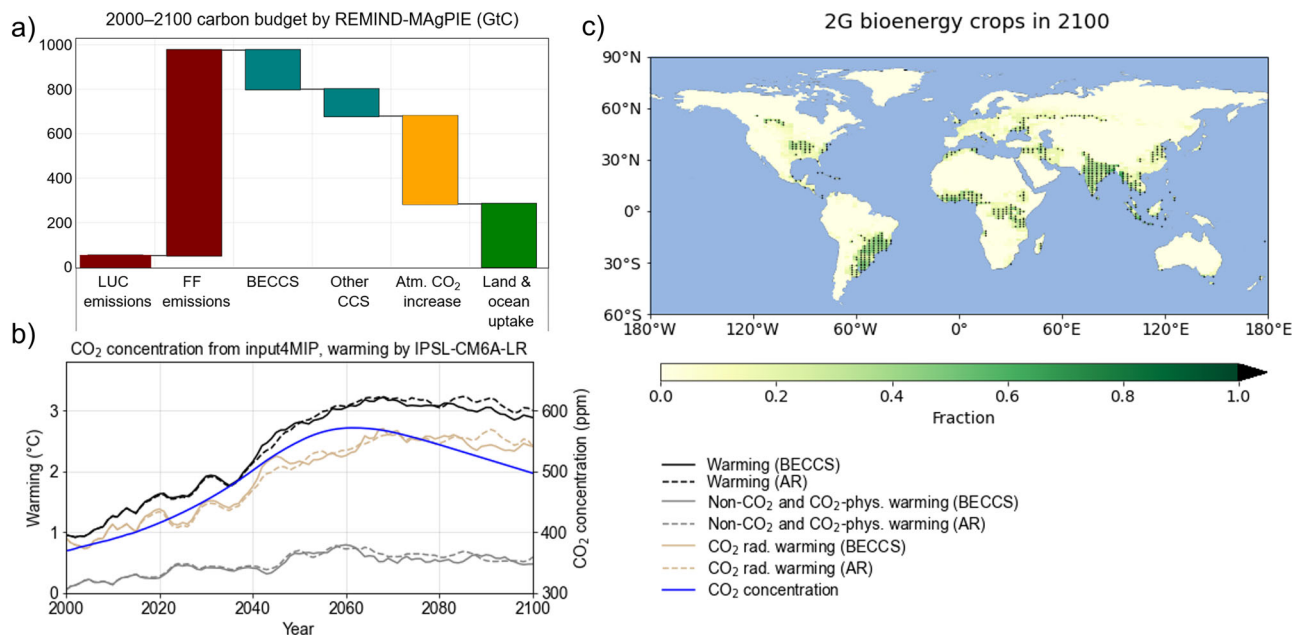


**Fig. 1** SSP5-3.4-OS simulated by REMIND-MAGPIE, LUH2, and IPSL-CM6A-LR. **a** Carbon budget (in GtC) for the 2000–2100 period estimated from REMIND-MAGPIE unharmonized emissions (dark red) and carbon capture and storage (teal), and atmospheric CO<sub>2</sub> increase (orange), land and ocean carbon uptakes (green) estimated from the mass balance conservation. **b** The CO<sub>2</sub> concentration (ppm) of input4MIPs (blue), and total (black), non-CO<sub>2</sub> and CO<sub>2</sub> physiological (grey), and CO<sub>2</sub> radiative (light brown) global mean surface temperature change relative to 1850–1899 baseline (°C) simulated by IPSL-CM6A-LR given as 5-year moving averages in standard BECCS (solid lines) and AR (dashed lines) experiments. **c** Spatial distribution of 2 G bioenergy crop cover in 2100 by LUH2, given as a fraction of a gridbox. Black dots indicate the gridboxes with over 20% of 2 G bioenergy crops in 2100.

reaching 0.9 °C. It steadily contributes  $0.7 \pm 0.1$  °C to warming over the 2040–2100 period. All contributors to warming vary temporally (and spatially) between the BECCS and AR experiments (Fig. 1b). The AR experiment gives comparable maximum GSAT and peak year with the BECCS experiment; however, the 2090–2100 mean GSAT is slightly higher (3.2 °C) than in the BECCS experiment.

In the high- and mid-latitude subregions of the Northern Hemisphere, the impacts of AR/BECCS allocation on surface climate are dominated primarily by radiative mechanisms, whereas in most subtropical and tropical subregions of the Southern Hemisphere, they are dominated by non-radiative mechanisms. Under SSP5-3.4-OS, BECCS (as opposed to AR) leads to more local warming in the Southern Hemisphere and cooling in the high latitudes (Fig. 2a–d). The radiative mechanisms, such as higher albedo that tends to cool climate locally, explain the local temperature differences over central North America and some parts of East Asia. In agreement with existing studies<sup>30</sup>, we show that allocation of the darker forest (compared to brighter bioenergy crops) leads to a decrease in the surface albedo, resulting in the higher net surface radiation in the boreal subregions (Fig. 2d). The non-radiative mechanisms, such as increased sensible heat fluxes and reduced canopy roughness that leads to increased aerodynamic resistance<sup>31</sup>, explain the local temperature differences in the semi-arid regions of eastern Latin America, central Africa, and India. In these areas, the expansion of bioenergy crops leads to local decreases in the surface relative humidity.

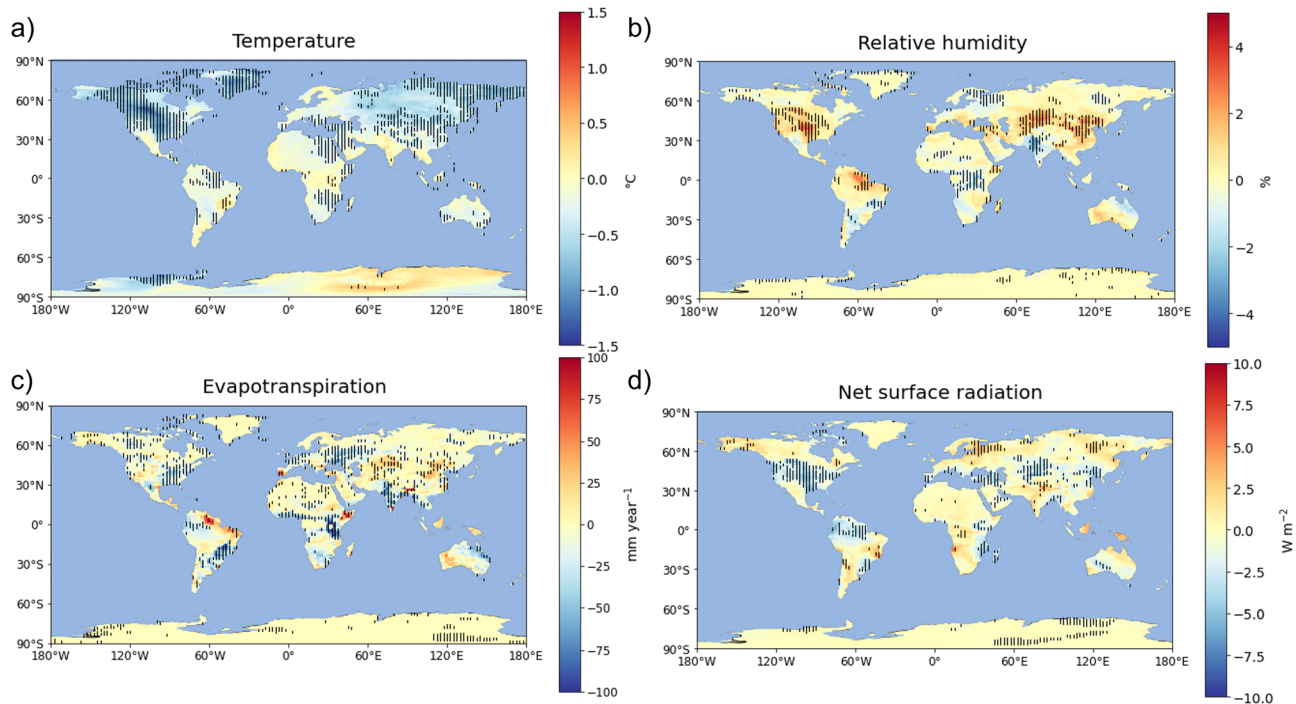
The global and subregional differences (defined using five macro-regions from the Representative Concentration Pathway models, Fig. S1) in biogeophysical variables do not saturate over time, at least during the study period (Supplementary Figs. S2–S5). Certain biogeophysical differences, such as lower evapotranspiration globally and in the Middle East and Africa region and lower net surface radiation in the OECD countries region in BECCS

compared to the AR experiment, cannot be explained by natural variability. Further analysis based on the multi-ensemble simulations is required to explain the temporal variation of these differences, considering the increase in land-use areas, the changes in crop yields, and forest carbon uptake.

We also examined how the physiological CO<sub>2</sub> forcing affects surface air temperature changes over the AR/BECCS allocated areas. To this end, we compared the fully coupled (COU) and biogeochemically-coupled (BGC) simulation outputs of AR and BECCS with the BGC and COU simulation outputs with land cover fixed to its 2040 distribution (Supplementary Fig. S6). Both physiological and biogeophysical effects of AR on temperature change are more pronounced than those in the BECCS experiment. This is due to the stronger coupling of the forest with the atmosphere, as compared to crop, which increases the effect of elevated CO<sub>2</sub> on reducing the total surface resistance.

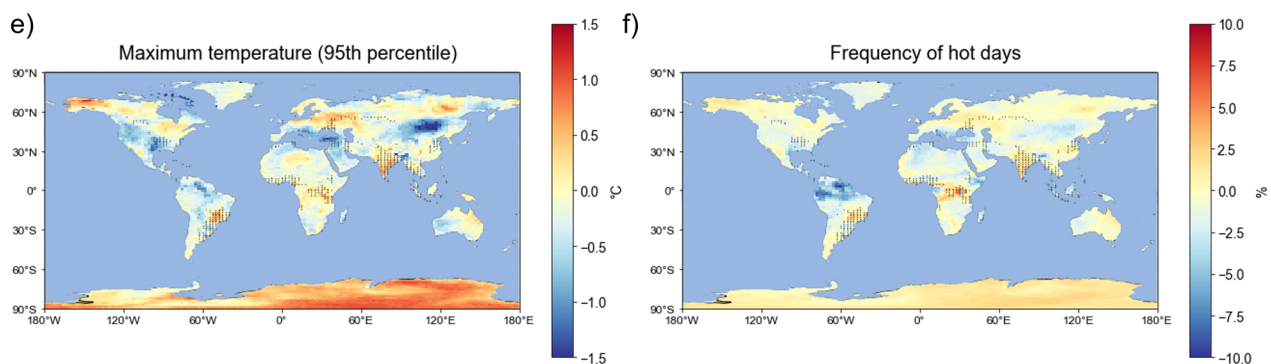
Our results shed light on the impact of the choice of two CDR methods on extreme heat events, defined via the 95<sup>th</sup> percentile of the maximum daily surface air temperatures (Fig. 2e–f). BECCS deployment leads to an increase in both the magnitude and frequency of extreme heat events in the target areas of the Southern Hemisphere, the low latitudes of the Northern Hemisphere, and Central Europe compared to AR. In Europe, these increases in heat extremes occur despite the cooling effect of bioenergy crops on mean surface temperature compared to AR. The design of this study does not allow disentangling local and non-local biogeophysical effects of BECCS and AR, and the analysis of the extreme events requires further consideration, e.g., by taking into account the joint temperature-humidity events<sup>34</sup>. The statistically significant differences in surface climate variables between the BECCS and AR experiments in the areas remote from their allocations imply an alteration of the large-scale atmospheric circulation (beyond the scope of the current study), which should also be considered in further analyses.

## Difference in 2081–2100 means between BECCS and AR simulations



Black lines correspond to significant differences according to Mann–Whitney U test ( $p$  value < 0.05)

## Difference in 2081–2100 hot extremes rel. to 1995–2014 between BECCS and AR simulations



Black dots indicate the gridboxes with over 20% of 2G bioenergy crops in 2100.

**Fig. 2** Spatial distributions of climate variables in BECCS and AR experiments. Differences in **a** surface air temperature (°C), **b** relative humidity (%), **c** surface evapotranspiration (mm year<sup>-1</sup>), and **d** net surface radiation (W m<sup>-2</sup>) averaged over 2081–2100 between the BECCS and AR experiments. Black vertical lines correspond to the gridboxes with a significant difference ( $p$ -value < 0.05) according to the Mann–Whitney U test. Differences in **e** daily maximum surface air temperature at 95<sup>th</sup> percentile (°C) and **f** frequencies of days with maximum temperature above 95<sup>th</sup> percentile (%) estimated in 2081–2100 rel. to 95<sup>th</sup> percentile of 1995–2014 baseline in BECCS and AR experiments. Black dots indicate the gridboxes with over 20% of 2G bioenergy crops in 2100. Positive values indicate larger values in the BECCS than in the AR experiment.

Here we show the potential regional impacts of the two CDR methods on the local climate. Radiative mechanisms in the biogeophysical effects cause local cooling (negative feedback), and thus benefits of BECCS on climate in most target areas of the northern high- and mid-latitudes, with the exception of Europe, where BECCS may lead to more heat extremes. Non-radiative mechanisms in the biogeophysical effects lead to local cooling (negative feedback), and thus benefits of AR on climate in the target areas of most tropical and subtropical latitudes of the Southern Hemisphere under the SSP5-3.4-OS scenario.

**Land-use change emissions.** There are several ways to estimate LUC emissions from Coupled Model Intercomparison Project

(CMIP6) ESM simulations<sup>4</sup>. We compared the IPSL-CM6A-LR LUC estimates via two approaches, namely (1) fLUC, i.e., via fLUC variable (net carbon mass flux into the atmosphere due to LUC excluding forest regrowth) diagnosed as an output of ESM, and (2) LU – noLU2040, i.e., the difference between the paired simulations, one with LUC and the other with land cover fixed to its 2040 distribution. The fLUC variable includes only the direct emissions that occur when a native ecosystem is converted to a new ecosystem such as BECCS, while the LU – noLU2040 allows the comparison of the potential carbon sink of the new ecosystem with that of the native ecosystem<sup>4,35</sup>. The 2040–2100 cumulative LUC emissions estimated by REMIND-MAGPIE are closest to those from the fLUC approach by IPSL-CM6A-LR in the BECCS experiment (Table 1, Supplementary Figure S7). However, unlike



**Table 1 2040–2100 LUC cumulative emissions (GtC) estimated using two approaches by IPSL-CM6A-LR and REMIND-MAGPIE.**

| Experiment | fLuc | LU–noLU 2040 | LUC by IAM | BECCS carbon removal by IAM |
|------------|------|--------------|------------|-----------------------------|
| BECCS      | 30.1 | 18.9         | 25.5       | 176                         |
| AR         | 15.9 | –47.6        |            |                             |
| BECCS – AR | 14.2 | 66.5         |            |                             |

Positive values indicate a source to the atmosphere. BECCS carbon removal not accounting for LUC estimated by the IAM is provided for reference.

the set of simulations with and without LUC, the fLuc-based estimates do not account for forest regrowth (particularly relevant for the AR experiment) and extra LUC emissions, such as the legacy of soil carbon from former lands on heterotrophic respiration and the loss of additional sink capacity. The simulation with BECCS leads to 66.5 GtC more LUC emissions than AR over the 2040–2100 period as obtained under the LU – noLU2040 approach (Table 1).

**Global land carbon fluxes and carbon cycle feedbacks.** LUC emissions associated with the large-scale bioenergy crop deployment lead to a decrease in the land carbon sink, as seen from the differences in Net Biome Production (NBP) (Fig. 3). In IPSL-CM6A-LR, NBP includes carbon sink accounting for nutrient limitation, harvest, and LUC emissions. Note, however, that the model version that we use does not have a fire module. The difference in NBP between BECCS and AR experiments reaches 66.5 GtC over 2040–2100 and can be fully explained by the LUC emissions, which include the loss of additional sink capacity.

Changes in NBP can be modulated by the carbon-concentration ( $\beta$ ) and carbon-climate ( $\gamma$ ) feedbacks. A combination of COU and BGC experiments using IPSL-CM6A-LR enables an analysis of these feedbacks on the NBP in BECCS and AR experiments (Fig. 3). The  $\beta$ -driven contribution to NBP can be estimated from the BGC experiment, and the  $\gamma$ -driven contribution is estimated from the difference between COU and BGC experiments. Note that although BGC simulations by design do not include CO<sub>2</sub> radiative forcing, they still include non-CO<sub>2</sub> and CO<sub>2</sub> physiological forcing that differ between BECCS and AR experiments (Fig. 1b). Thus, BGC simulations include  $\beta$  feedback and non-CO<sub>2</sub> and CO<sub>2</sub> physiological forcing-driven  $\gamma$  feedbacks, and COU simulations further include CO<sub>2</sub>-driven  $\gamma$  feedback in addition to all feedbacks considered in BGC simulations. Due to the experiment design described above, the contributions of  $\beta$  feedback cannot be separated from those of  $\gamma$  feedbacks driven by non-CO<sub>2</sub> and CO<sub>2</sub> physiological forcing. In this study, we discuss  $\beta$  and  $\gamma$  feedbacks, taking into account the contributions of non-CO<sub>2</sub> and CO<sub>2</sub>-driven  $\gamma$ , which account for nearly 20% of the total  $\gamma$ .

Both  $\beta$  and  $\gamma$  feedbacks are stronger for forests than for bioenergy crops because of the larger biomass (in the forest) exposed to the changes in the CO<sub>2</sub> concentration and climate. During the ramp-down phase of the temperature overshoot scenarios, as in this study, the decrease in surface temperature lags behind that of CO<sub>2</sub> due to the inertia of the climate system. These changes are reflected in two carbon fluxes, Net Primary Production (NPP) and Heterotrophic Respiration (Rh), which comprise NBP (although not completely). NPP peaks earlier than Rh due to its primary dependence on CO<sub>2</sub>, albeit with regional variations<sup>28</sup>. Analysis of the slopes of linear regressions of carbon fluxes and surface climate variables (Supplementary Figure S8) and the correlation coefficients between them (Supplementary Figs. S9–S11) during the 2061–2100 period enables further

examination of the drivers of the carbon flux changes in two experiments. In the South American new land use allocation areas, NBP decreases more in the AR experiment rather than in the BECCS experiment because of a relatively larger decrease in NPP than in Rh in the AR experiment. In this region, NPP is positively correlated with the precipitation and relative humidity, as well as CO<sub>2</sub>, and negatively correlated with surface air temperature. Thus, a lag in temperature decrease behind that of CO<sub>2</sub> concentration and increased water stress may lead to greater losses in AR areas compared to bioenergy crops. In the northern mid-to-high latitude allocation areas, the climate impacts on the carbon fluxes are regionally diverse. In the North American target areas, a larger decrease in NBP in AR compared to the BECCS experiment is likely due to a larger decrease in NPP due to lower relative humidity, while in Europe, a smaller NBP decrease compared to the BECCS experiment is driven by both a positive correlation with surface air temperature and higher humidity. These findings are consistent with recent observationally-based studies showing an increase in tree mortality due to increased atmospheric water stress and nutrient limitation under elevated CO<sub>2</sub> concentration in tropical forests and questioning the simulated increase in total growth under warmer temperatures in temperate deciduous trees<sup>36,37</sup>.

The carbon-concentration and carbon-climate feedbacks have smaller effects in the BECCS experiment. LUC emissions override  $\beta$ -driven increases in the carbon uptake in BECCS so that the BGC experiment results in decreased carbon uptake in some allocated areas of Latin America and Africa. Globally, the LUC-associated carbon losses are outweighed by the positive impacts of the  $\gamma$  feedback. This is apparent in the high northern latitudes, where the  $\gamma$  feedback increases the carbon removal of BECCS and AR in the ‘colder’ subregions of the OECD countries in 1993 and Reforming economies under the SSP5-3.4-OS (Fig. 3g). Nevertheless, the bioenergy crop-concentrated areas (gridboxes that have >20% bioenergy crops) lose 4.0 GtC additional sink via the  $\gamma$  feedback (Supplementary Figure S12). Besides, the  $\gamma$  feedback considerably limits land carbon uptake in Latin America, the Middle East, and Africa subregions in both BECCS and AR experiments. Planting crops (rather than forests) in the target areas of low latitudes prevents the carbon stored in the biomass from being exposed to the  $\gamma$  feedback but also leads to a smaller  $\beta$ -driven increase in the land sink due to the shorter turnover time of carbon in crops compared to forests.

The land component of the IPSL-CM6A-LR model does not have a fire module, and the impact of droughts is limited to NPP with no climate-induced increase in vegetation mortality, especially in the AR experiment. Previous studies show that climate-induced droughts and fires may turn forests from carbon sinks to sources directly via tree mortality and lead to the increased crop yields losses<sup>18,38,39</sup>. One study estimated that inclusion of a fire module to the biosphere model may reduce the global land carbon sink by 20% during the historical period<sup>40</sup>. Thus, the  $\gamma$  feedback may be underestimated in the AR and BECCS experiments. Besides, we investigated a future scenario that involves a temperature overshoot of 3.4 °C relative to the 1850–1899 levels. We speculate that a higher GSAT increase may lead to larger carbon-climate feedbacks and, thus, further losses of sequestered carbon by both BECCS and AR, which vary regionally and are not currently accounted for by IAMs<sup>3</sup>.

The impacts of bioenergy crop deployment or AR are not limited to the carbon cycle. Bioenergy crop deployment affects the surface energy budget and the hydrological cycle as well, leading to increased runoff in all areas considered except b (where the effects are heterogeneous) and, thus, potentially leading to increased water scarcity (Supplementary Fig. S13). The utilized ESM did not consider irrigation of bioenergy crops, which could

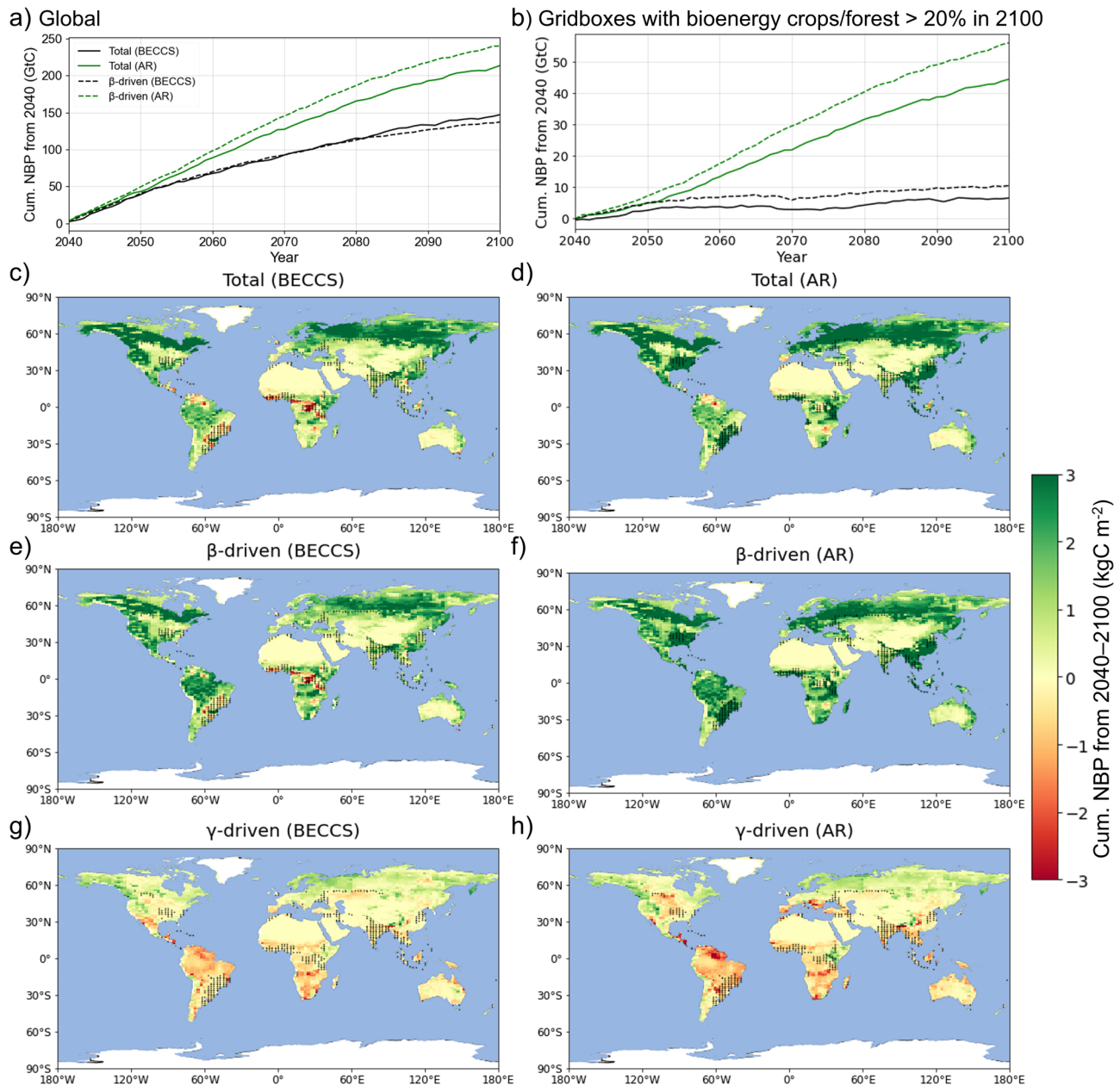


**Fig. 3 Temporal and spatial distributions of land carbon flux.** Time evolution of the cumulative NBP flux (GtC, positive to land) over the 2040–2100 period **a** on a global scale and **b** over the regions dominated by 2 G bioenergy crops or forest (gridboxes that include >20% of new bioenergy crops/forest in 2100). NBP estimates are given for the fully coupled simulations (solid lines) and simulations that do not consider climate feedbacks (dashed lines) in the BECCS (black) and AR (green) experiments. Spatial distributions of the cumulative **c, d** NBP and the respective contributions of **e, f**  $\beta$  and **g, h**  $\gamma$  feedbacks over the 2040–2100 period in the **c, e, g** BECCS and **d, f, h** AR experiments. Black dots indicate the gridboxes with over 20% of 2 G bioenergy crops in 2100.

increase the carbon removal of bioenergy crops but also increase water stress in the region<sup>41,42</sup>.

**Global and regional carbon budgets under SSP5-3.4-OS variants.** Under SSP5-3.4-OS variants of land cover scenarios, BECCS results in higher carbon removal than AR, but the benefits of BECCS over AR vary subregionally (Figs. 4–6). Ecosystem carbon storage, especially in the biomass pool (wood, leaves, and roots), is greater in AR than in the BECCS experiment. Carbon residence time is longer in forests than in short BECCS vegetation, where crop soil decomposition is faster than in other land-use tiles (see Methods). Although the utilized ESM does not explicitly model bioenergy crops, our offline simulations based on

conventional crops with additional aboveground biomass harvest and its impacts on soil carbon show that the higher yields of the bioenergy crops partially compensate for the faster carbon turnover in the soil (we assume that 80% of NPP is harvested). The higher NPP in the BECCS compared to the AR experiment also confirms the satisfactory performance of the bioenergy crop system simulation (Supplementary Fig. S14). The annual mortality of the forest, modelled via the input of leaves and branches into the litter pool, is comparable to the input of 2 G crop residues into the soil pool. All of this results in only a tiny difference in the soil carbon pool between the AR and BECCS experiments. The largest carbon removal benefits of BECCS over AR are in the semi-arid subregions of Latin America and Central Africa.

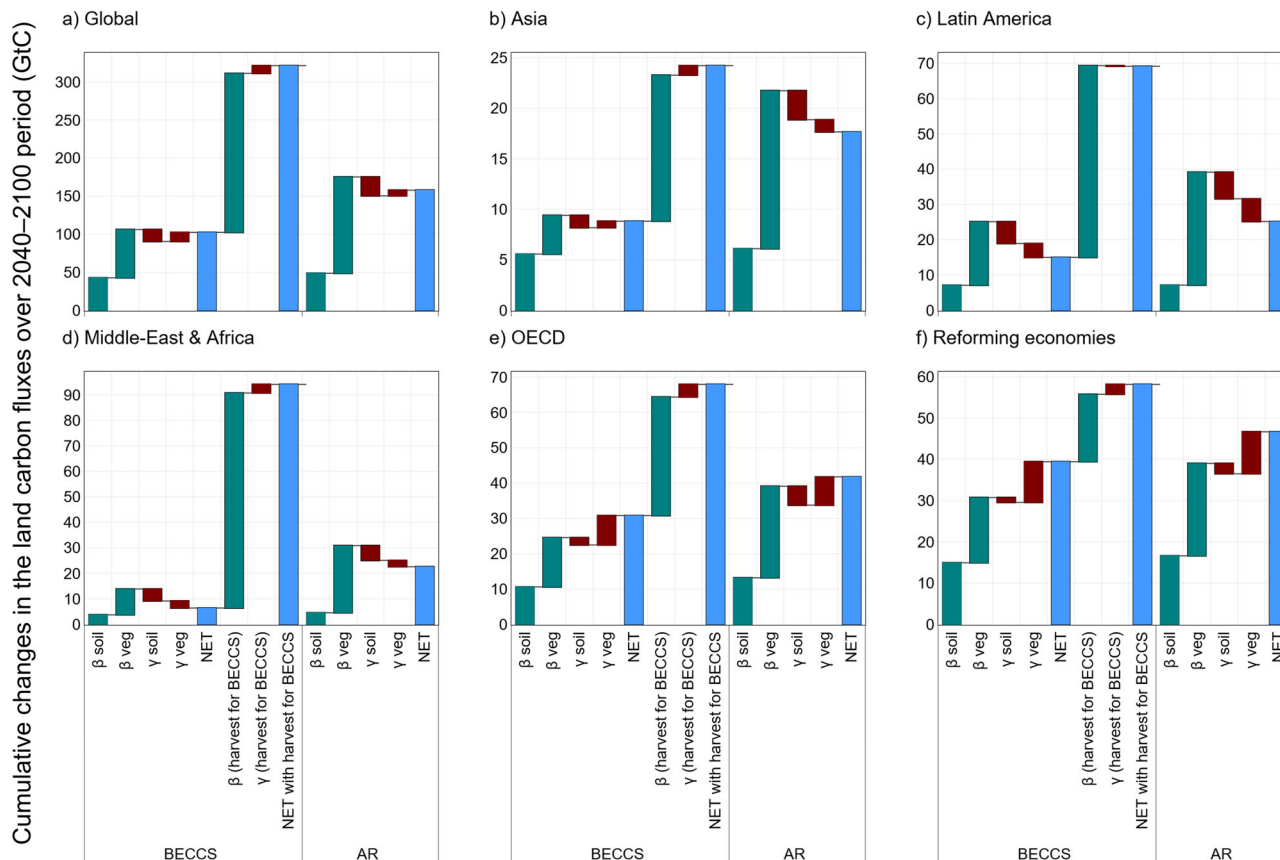


**Fig. 4** Changes in the  $\beta$ - and  $\gamma$ -driven contributions to the land carbon budget. The  $\beta$ -driven (green) and  $\gamma$ -driven (dark red) contributions to net biome production (blue) and biomass harvest for BECCS carbon removal in the BECCS and AR SSP5-3.4-OS experiments over the 2040–2100 period globally **a** and regionally **b–f**. LUC emissions are included in the  $\beta$ - and  $\gamma$ -driven contributions. Harvest for BECCS stands for harvested biomass for BECCS carbon removal (prior to multiplying by permanently captured carbon fraction). A positive change means more carbon is stored in the soil, vegetation, or geological reservoirs.

However, these areas do not have the biogeophysical benefits of cooling by BECCS. Deployment of BECCS in these areas may lead to the disadvantages of non-radiative climate effects and an increase in extreme heat events.

The advantages of BECCS over AR are contingent on the assumptions made about future technological progress to increase the fraction of carbon that is captured and stored permanently. Although, on a global scale, a fraction of around 25% already results in higher carbon removal by BECCS compared to the AR experiment (Supplementary Figure S15), this may not be sufficient in some regions, such as parts of Europe and East Asia (Fig. 6). The relatively low carbon removal of bioenergy crops in the allocated areas of these regions may be partly explained by the higher temperatures and lower surface humidity, as well as the increased frequency of extreme heat events (Fig. 2). In these regions, the carbon loss from LUC may exceed the carbon removal by bioenergy crops. To achieve more carbon removal by BECCS than by AR by 2100, the permanently captured carbon fraction should be larger than 20% in Latin America, the Middle East, and Africa, larger than 30% in OECD countries, larger than 40% in Reforming economies, and larger than 60% in Asia (Supplementary Fig. S15). In this study, we focus on natural AR by planting the forest types that are native to the allocated area. Thus, we do not apply forest harvesting and do not consider the use of forest plantations. A pragmatic implementation of AR would involve some timber harvesting for manufacturing bio-based materials, which can provide additional long-term carbon storage in addition to the benefits of building housing and

infrastructure and substituting for the construction-related GHGs emissions<sup>43,44</sup>. AR with regular harvesting could therefore be even more competitive than BECCS in terms of the amount of carbon removal achieved.

The temporal dimension of carbon removal is another important aspect. AR captures carbon faster in the early successional stage (young forest) and slows down as the forest ages. The carbon removal by BECCS may increase in the future with technological development (not considered in this study). A comparison of the interannual variation of changes in the land carbon budget shows that there is only a little difference between the carbon removals by the two methods globally until the 2070s (Fig. 5j–l). In the long term, BECCS is more beneficial for carbon removal globally and regionally, with the exception of Asia, where only permanently captured carbon fraction larger than 60% leads to more carbon removal by BECCS than AR by 2100. In the short term (20–30 years after deployment), AR may be as beneficial or more beneficial than BECCS in all subregions with the exception of the Middle East and Africa. The allocation of land areas to BECCS and AR should consider this temporal change in carbon removal, bearing in mind that many countries aim to achieve carbon or GHG neutrality by the 2050s–2070s.

**Limitations and future perspectives.** This study presents an attempt to explicitly model two CDR methods under a future SSP5-3.4-OS mitigation pathway within a state-of-the-art ESM accounting for the effects of biogeochemical and biogeophysical feedbacks in allocated areas at global and regional scales. We



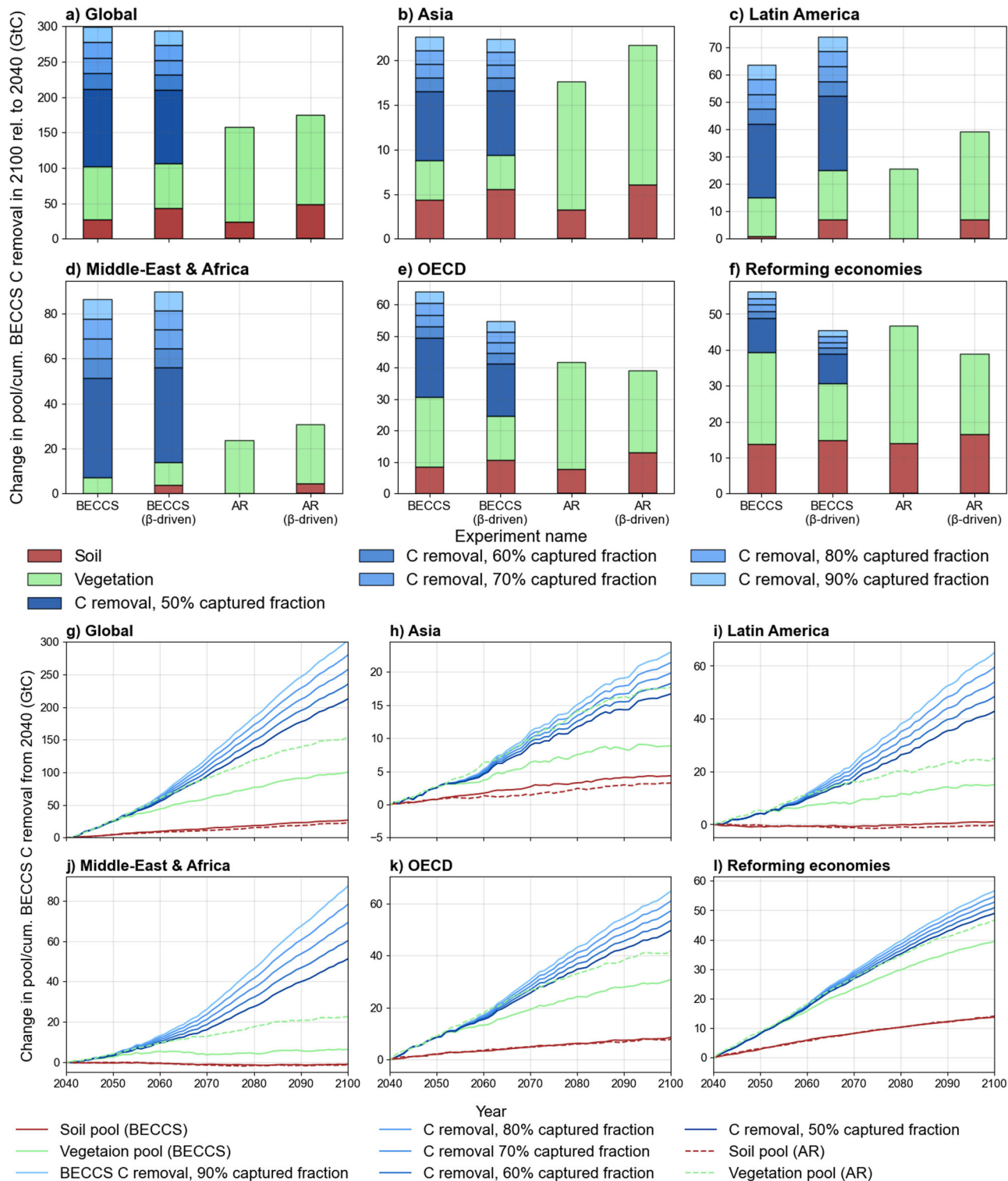


**Fig. 5 Changes in the land carbon budget, including BECCS carbon removal.** Changes in the soil (brown), vegetation (green) carbon pools, and BECCS carbon removal, assuming permanently captured carbon fraction from 50 to 90% (light blue to dark blue) in the BECCS and AR SSP5-3.4-OS experiments from the fully coupled simulations and simulations that do not consider climate feedbacks over the 2040–2100 period globally **a** and regionally **b–f**, and the temporal changes (stacked) in contributors to land carbon budget globally **g** and regionally **h–i**. Regional allocation of carbon removal by BECCS refers to the location of biomass extraction. LUC emissions are accounted for in the estimates.

discussed the advantages and disadvantages of allocating bioenergy crops and forests in different subregions to increase their carbon removals under future mitigation strategies.

In the SSP5-3.4-OS land-use scenario, the allocation of bioenergy crops was prioritized in so-called degraded areas with

low soil and biomass carbon content<sup>4</sup>. However, the REMIND-MAGPIE that was used to develop the SSP5-3.4-OS land use scenario made a first-order decision to allocate bioenergy crops in areas that are optimal for BECCS based on socioeconomic and climatic factors. On the one hand, this may have influenced our



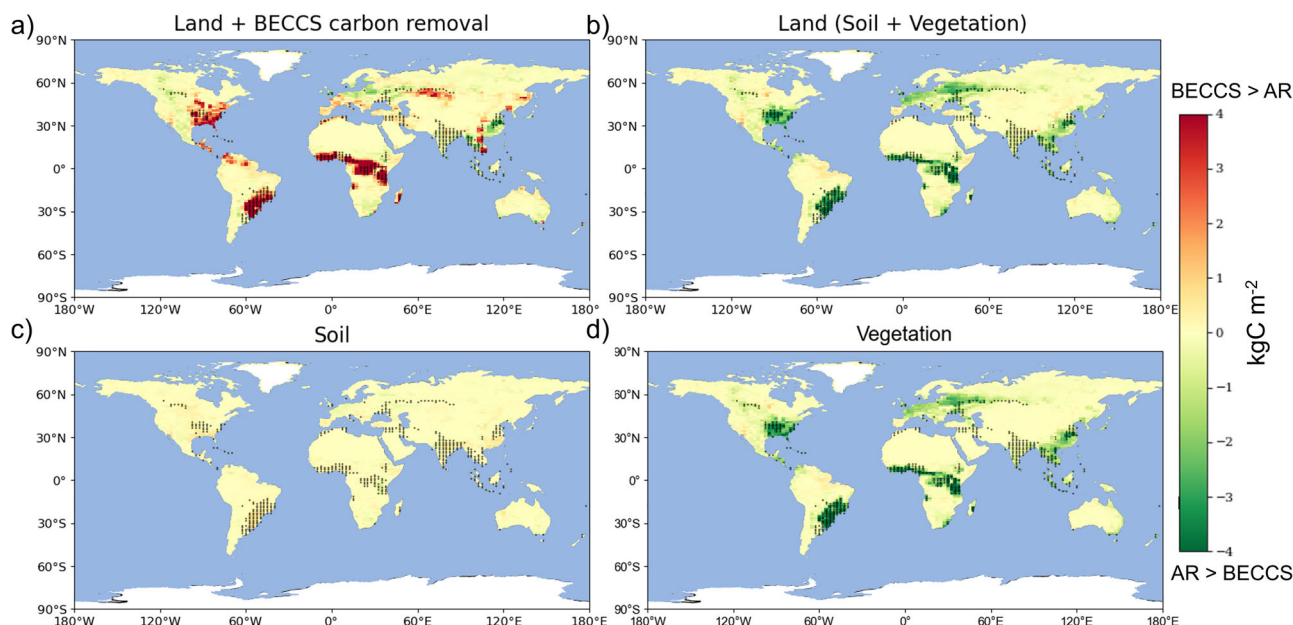


**Fig. 6** Spatial distributions of net change in land carbon pools. Distribution of the net change in **a** total land pool and carbon removal by BECCS with permanently captured carbon fraction of 50%, **b** total land, **c** soil, and **d** vegetation carbon pools between the BECCS and AR experiments in 2100. Positive values indicate larger values in the BECCS than in the AR experiment. The black dots indicate the gridboxes with over 20% of 2 G bioenergy crops in 2100. The carbon removal indicates the location of biomass extraction. LUC emissions are accounted for in the estimates.

comparison between the two climate mitigation methods and may have favored BECCS over AR, as discussed further in Supplementary Text S1 and Figures S16–S20. We found no large differences with our results when looking only at the target areas where the IAM allocated only BECCS or both BECCS and AR. However, the potential benefits for carbon removal by BECCS over AR may be reduced when considering only those target areas, where the IAM assigned AR. On the other hand, the definition of degraded land by MAGPIE and LUH2 for BECCS allocation may differ considerably from observationally based data sets on available marginal land for 2 G crops<sup>2</sup>.

The SSP5-3.4-OS scenario includes large increases and decreases in the atmospheric concentration of methane<sup>10</sup>. Methane is a major contributor to tropospheric ozone, which can damage crops and vegetation, thereby reducing carbon uptake. However, the version of the ESM used in this study did not account for these effects. Similarly, the model does not consider irrigation of bioenergy crops, which may increase the carbon removal by BECCS but may also increase the water stress in the allocated areas. Furthermore, the lack of fire and drought mortality module in the ESM presumably led to under-estimation of the carbon–climate feedback, especially in the AR experiment. In addition, the choice of mitigation method may have a negative impact on the protection of the local biodiversity<sup>42</sup>. Further consideration is needed for an integrated assessment of BECCS and AR not only in terms of carbon sequestration and climate but also in terms of biodiversity protection, ecosystem services, and environmental sustainability.

To further complement our findings, we call for more national-scale studies<sup>45</sup> to investigate CDR methods with an adequate level of process details. Future studies should also explore CDR methods in emission-driven simulations in order to explore biogeochemical and biogeophysical feedbacks<sup>46</sup> more interactively.

Our results are based on only one model, indicating the need for more thorough investigations using a suite of models integrating a bioenergy crop module. This also highlights the need to explicitly include various CDR methods in ESMs, in order

to better assess CDR methods required to meet the Paris Agreement targets. Furthermore, we suggest that future studies compare the impacts of BECCS/AR allocation on other Earth System feedbacks and tipping points and include a quantitative comparison of the biogeochemical and biogeophysical feedbacks.

## Methods

**Earth system model.** We use Version 6 of the Institut Pierre-Simon Laplace (IPSL) low-resolution ESM, IPSL-CM6A-LR, developed in the runup for the sixth phase of the CMIP6<sup>47</sup>. This ESM comprises the LMDZ atmospheric model Version 6 A-LR, the NEMO oceanic model Version 3, and the ORCHIDEE land surface model Version 2.0 with a  $144 \times 143$ -grid spatial resolution. ORCHIDEE is a process-based terrestrial biosphere model that calculates energy, water, and carbon fluxes between the land surface and the atmosphere. The current CMIP6 version does not include a fire module and does not account for crop irrigation. Disturbances include biomass harvesting. In the model, droughts reduce NPP but do not increase mortality. Nutrient limitation of photosynthesis is modelled via a downregulation mechanism through a logarithmic function at  $\text{CO}_2$  concentrations above 380 ppm. Vegetation properties are defined by 15 different plant functional types (PFTs). Among them, forest is represented by eight PFTs, short vegetation – by six PFTs, including C3 and C4 grasses and crops, and one PFT stands for bare soil. These PFTs are integrated into the land-use tiles, namely crops and primary and secondary land, represented at a subgrid-scale. The carbon pools include vegetation, litter, and soil pools, with soil divided into fast, medium, and slow reservoirs. The carbon turnover times are 1.5 years for fast, 25 years for medium, and 1000 years for slow pools.

**SSP5-3.4-OS scenario.** The SSP5-3.4-OS (Fig. 1) is an overshoot pathway developed by the Regional Model of Investment and Development—Model of Agricultural Production and its Impacts on the Environment (REMIND-MAGPIE) model. This scenario follows the high-emission SSP5-8.5 scenario until 2040<sup>8,10,46</sup>. It then assumes aggressive mitigation policies after 2040 dominated by an expansion of 2 G bioenergy crops for BECCS prioritized over low-carbon-content lands, such as pastures and some existing croplands<sup>4,48</sup>. The delayed mitigation leads to an overshoot beyond the  $2^\circ\text{C}$  warming limit of the Paris Agreement, with a total radiative forcing of  $3.4 \text{ W m}^{-2}$  in 2100. In SSP5-3.4-OS, the cumulative net carbon emissions from REMIND-MAGPIE over the 1850–2100 period reach 1134 GtC, including 905 GtC net fossil fuel (FF) and 229 GtC net LUC emissions (Fig. 1a). The FF emissions include (and are offset by) CCS, which is implemented from 2010. CCS reaches a cumulative net amount of nearly 297 GtC, including BECCS. BECCS dominates carbon removal, accounting for 176 GtC of  $\text{CO}_2$  removed from the atmosphere by 2100. Figure 1a shows the carbon budget (GtC)<sup>49</sup> estimated from the cumulative land-use ( $E_{\text{LUC}}$ ) and fossil fuel (FF) emissions ( $E_{\text{FF}}$ ) offset by CCS, including BECCS, that are partitioned between atmospheric  $\text{CO}_2$

growth ( $G_{Atm-re}$ ) and land and ocean carbon uptakes ( $F_{Land}$  and  $F_{Ocean}$ ), according to the following equation:

$$E_{FF} + E_{LUC} - CCS = F_{Land} + F_{Ocean} + G_{Atm-re} \quad (1)$$

Here we estimated the left-hand side of the equation from the unharmonized REMIND-MAGPIE emissions and then used the input4MIPs CO<sub>2</sub> concentration to derive the atmospheric CO<sub>2</sub> growth on the right-hand side. Land and ocean carbon uptakes were assumed from the mass balance conservation.

The spatially explicit data on bioenergy crop yields, LUC emissions, and their biogeochemical and biogeophysical constraints for REMIND-MAGPIE come from the managed planetary land surface model, Lund-Potsdam-Jena managed Land (LPJmL)<sup>50,51</sup>. Then, the scenario data on the global and macroregional scales are produced and published from REMIND-MAGPIE, consistently with other scenarios<sup>52,53</sup>. The Harmonization of Global Land-Use Change and Management version 2 (LUH2) project provides maps of land use and land cover changes in a coherent gridded format as required for ESMs<sup>48</sup>.

**SSP5-3.4-OS-AR experiment.** We design a variant of the standard SSP5-3.4-OS scenario (with BECCS), referred to as SSP5-3.4-OS-AR, whereby the areas of the bioenergy crop deployment are converted to the forest instead (Supplementary Fig. S21). The bioenergy crop deployment under SSP5-3.4-OS is dominated by C4 crops, which appear mainly after 2040. We replace the transitions of any PFT to C4 crops after 2040 with those to forest, e.g., instead of a 1% increase in C4 crops, we apply a 1% increase in the forest. IPSL-CM6A-LR has eight forest types, so the forest type for AR in a given gridbox is determined proportionally to the forest PFT that already exists in the gridbox. If no forest exists in the gridbox (this situation can occur only in arid areas), then the C4 crop is deployed in SSP5-3.4-OS-AR as in the standard simulation. In the rare cases, when forest is converted to the C4 crop in the standard SSP5-3.4-OS scenario, the subgrid remains forest in the SSP5-3.4-OS-AR scenario. Supplementary Fig. S21 demonstrates the differences in the cropland and forest covers in the two experiments.

**Estimation of biogeophysical effects.** The following climate variables were considered in this study: surface air temperature (°C), relative humidity (%), evapotranspiration (mm year<sup>-1</sup>) (variable names are *tas*, *hurs*, *evsplt* in CMIP6), and net surface solar radiation (W m<sup>-2</sup>), estimated as a difference between incoming and outgoing solar radiation (variable names are *rsds* and *rsus* in CMIP6). Significant differences in mean climatologies were evaluated according to the Mann-Whitney U test. This test was selected because of the small sample size ( $n = 20$ ) of the variable that is not distributed normally. The analysis of the hot extremes was carried out based on the daily maximum temperatures (°C).

**Estimation of carbon removal by BECCS.** IPSL-CM6A-LR does not treat bioenergy crops explicitly but instead uses a generic crop vegetation type that is parameterized with 20% and 40% higher soil carbon turnover than natural PFTs for C3 and C4 crops, respectively. The crop harvest is 45% of the aboveground net primary production (NPP) of crops by default; it is harvested and stored in a separate reservoir where it is respired within one year. To estimate the carbon removal by BECCS from IPSL-CM6A-LR outputs, we assume that all croplands deployed after 2040 correspond to 2 G bioenergy crops devoted to BECCS<sup>4,48</sup>. We estimate the NPP of the croplands that appear after 2040 using subgrid information (Supplementary Fig. S22). We use a higher harvest index than in a standard IPSL-CM6A-LR simulation, assuming that 80% of the total NPP of bioenergy crops is harvested so that a larger part of the biomass, including by-products and wastes, can be utilized. The higher potential yields of 2 G bioenergy crops compared to conventional crops have been discussed in the previous studies<sup>2,54,55</sup>. Re-scaling harvested biomass over bioenergy crop areas requires re-scaling the soil carbon pools of these areas. While in the standard simulation, 55% of aboveground crop NPP goes to the soil, with our revised estimate of harvest as 80% of NPP, only 20% of NPP can enter the soil carbon pools as litter. Note that the changes are applied only to the soil 'active carbon' layer (comprising fast, medium soil, and litter pools in IPSL-CM6A-LR) of bioenergy crops because the passive (slow) soil pool that has a turnover time of 1,000 years stays nearly constant. The carbon in soil active layer of cropland tiles that appear after 2040 is scaled with a 20 to 55% ratio. The re-scaling results in a cumulative difference of 41 GtC in harvest over the 2040–2100 period and a difference of 4 GtC in the 2100 soil carbon pool. We evaluated the bioenergy crop yields against observations<sup>56</sup> (Supplementary Fig. S23). To do this, we compared annual harvested biomass (kgC m<sup>-2</sup>) converted to crop yield (tDM ha<sup>-1</sup>) with the observations of 2 G bioenergy crops (miscanthus, switchgrass, or grass mixture) at 119 sites in a given year. Our simple offline simulations of bioenergy yield give satisfactory estimates, although slightly overestimating the observational based 2 G bioenergy yield.

We introduce a permanently captured carbon fraction to estimate carbon removal from the harvested biomass in bioenergy crops. According to techno-economic studies, it may vary between 50% and 90% and depends on the biofuel type, region, storage capacity, technological progress, etc.<sup>3,51</sup>. We apply a range of CCS factors and compare them to the estimates by REMIND-MAGPIE. The proposed simple approach allows us to obtain a first-order estimate of the carbon removal in 2 G bioenergy crops.

In addition to fully coupled simulation (COU), we perform a biogeochemically-coupled (BGC) SSP5-3.4-OS-afforestation simulation, where only the biogeochemical impact of atmospheric CO<sub>2</sub> concentration, and not the radiative impact, is accounted for<sup>28,57</sup>. The combination of COU and BGC simulations is used to investigate the carbon-climate feedbacks. Note that the radiative impact of nonCO<sub>2</sub> GHGs is still present in BGC simulations. The nonCO<sub>2</sub>-driven GSAT increase relative to the 1850–1899 baseline reaches its maximum of 0.9 °C in the early 2030 s from standard (with BECCS) SSP5-3.4-OS BGC simulation. This non-CO<sub>2</sub>-driven GSAT increase is equally present in both BECCS and AR experiments, but it may lead to varying carbon-climate feedbacks under two land-use maps.

IPSL-CM6A-LR can reproduce the estimates of BECCS' carbon removal by the IAM REMIND-MAGPIE that developed the SSP5-3.4-OS pathway on a global scale with the 179 GtC carbon removal by 2100 (against 176 GtC by REMIND-MAGPIE) when assuming a permanently captured carbon fraction of 80% (Fig. 1a). The permanently captured carbon fraction converts harvested biomass in bioenergy crops to the carbon removal by BECCS and may vary between 50% and 90% and depends on the biofuel type, region, storage capacity, technological progress, etc., according to techno-economic studies<sup>3,51</sup>. Regionally, IPSL-CM6A-LR estimates lower carbon removal by BECCS in Asia and Organisation for Economic Co-operation and Development (OECD) regions and higher carbon removal elsewhere than those from REMIND-MAGPIE under the range of permanently captured carbon fractions (50 to 90%). These differences in carbon removal by IPSL-CM6A-LR and REMIND-MAGPIE are due to discrepancies in the cropland area change between REMIND-MAGPIE and IPSL-CM6A-LR (Supplementary Fig. S24). The discrepancies emerge in the harmonization process of converting the land-use data from the IAM into LUH2 and then into the ESM<sup>4</sup>. LUH2 and IPSL-CM6A-LR are consistent in their estimates of temporal cropland area changes, but both deviate from the estimates by REMIND-MAGPIE. Discrepancies can also be seen in the regional estimates of the BECCS carbon removal rates. Yet, not only BECCS but also vegetation and soil carbon content estimated by the IAM and ESM perhaps differ (such data are not provided by IAMs). On the one hand, the differences in LUC emissions associated with land conversion to BECCS directly impact the total emissions of the given SSP scenario. On the other hand, the land cover differences impact the land carbon sink. More spatially explicit and detailed (e.g., gross emissions in addition to net emissions) information from the IAM scenario would enable a deeper understanding of this SSP pathway.

REMIND-MAGPIE provides low geographic details regarding the allocation of bioenergy crops and the types of crops and bioenergy so that its estimates are only available over five macro-regions<sup>52,53</sup>. At the same time, because IPSL-CM6A-LR lacks a dedicated representation of bioenergy crops, the estimated carbon removal by BECCS is contingent on the assumptions for the assumed harvest index and permanently captured carbon fraction. IPSL-CM6A-LR does not consider the permanently captured carbon fraction increase with technological progress, type of biofuel, and regional differences in various socioeconomic variables, technology availabilities, and policy frameworks included in REMIND-MAGPIE. These differences in the model representations need to be considered in interpreting the results.

## Data availability

The data from the CMIP6 simulations are available from the CMIP6 archive: <https://esgf-node.llnl.gov/search/cmip6><sup>58</sup>, the LUH2 data from <https://luh.umd.edu/data.shtml><sup>59</sup>, and the IIASA database via <https://tntcat.iiasa.ac.at/SpDb/dsd?Action=htmlpage&page=2052>. The data necessary to reproduce the figures are stored in the Zenodo archive <https://zenodo.org/record/7933146>.

## Code availability

The data was analyzed using CDO<sup>60</sup>. Code for reproducing the main plots of the manuscript is publicly available at <https://zenodo.org/record/7933146>.

Received: 6 October 2022; Accepted: 26 May 2023;

Published online: 29 June 2023

## References

1. Tanaka, K. & O'Neill, B. C. The Paris Agreement zero-emissions goal is not always consistent with the 1.5 °C and 2 °C temperature targets. *Nat. Clim. Change* **8**, 319–324 (2018).
2. Li, W. et al. Bioenergy crops for low warming targets require half of the present agricultural fertilizer use. *Environ. Sci. Technol.* **55**, 10654–10661 (2021).
3. Strefler, J. et al. Carbon dioxide removal technologies are not born equal. *Environ. Res. Lett.* **16**, 074021 (2021).
4. Melnikova, I. et al. Impact of bioenergy crops expansion on climate-carbon cycle feedbacks in overshoot scenarios. *Earth System Dyn.* **13**, 779–794 (2022).

5. Bachu, S. Sequestration of CO<sub>2</sub> in geological media: criteria and approach for site selection in response to climate change. *Energy Convers. Manag.* **41**, 953–970 (2000).
6. Longato, D., Gaglio, M., Boschetti, M. & Gissi, E. Bioenergy and ecosystem services trade-offs and synergies in marginal agricultural lands: a remote-sensing-based assessment method. *J. Cleaner Product.* **237**, 117672 (2019).
7. Milner, S. et al. Potential impacts on ecosystem services of land use transitions to second-generation bioenergy crops in GB. *GCB Bioenergy* **8**, 317–333 (2016).
8. Kriegler, E. et al. Fossil-fueled development (SSP5): an energy and resource intensive scenario for the 21st century. *Glob. Environ. Change* **42**, 297–315 (2017).
9. Hurtt, G. et al. Harmonization of global land use scenarios (LUH2): historical v2.1h 850–2015. <https://doi.org/10.22033/ESGF/input4MIPs.1127> (2017).
10. Meinshausen, M. et al. The shared socio-economic pathway (SSP) greenhouse gas concentrations and their extensions to 2500. *Geosci. Model Dev.* **13**, 3571–3605 (2020).
11. Brinkman, M. L. J., Wicke, B., Faaij, A. P. C. & van der Hilst, F. Projecting socio-economic impacts of bioenergy: current status and limitations of ex-ante quantification methods. *Renew. Sustain. Energy Rev.* **115**, 109352 (2019).
12. Lenton, T. M. The potential for land-based biological CO<sub>2</sub> removal to lower future atmospheric CO<sub>2</sub> concentration. *Carbon Manag.* **1**, 145–160 (2010).
13. Fargione, J., Hill, J., Tilman, D., Polasky, S. & Hawthorne, P. Land clearing and the biofuel carbon debt. *Science* **319**, 1235 (2008).
14. Wang, J. et al. Temperature changes induced by biogeochemical and biophysical effects of bioenergy crop cultivation. *Environ. Sci. Technol.* **57**, 2474–2483 (2023).
15. Fridahl, M. & Lehtveer, M. Bioenergy with carbon capture and storage (BECCS): Global potential, investment preferences, and deployment barriers. *Energy Res. Soc. Sci.* **42**, 155–165 (2018).
16. Smith, P. et al. Biophysical and economic limits to negative CO<sub>2</sub> emissions. *Nat. Clim. Change* **6**, 42–50 (2016).
17. Smith, S. M. et al. *The State of Carbon Dioxide Removal - 1st Edition*. <https://doi.org/10.17605/OSF.IO/W3B4Z> (2023).
18. Anderegg, W. R. L. et al. Climate-driven risks to the climate mitigation potential of forests. *Science* **368**, eaaz7005 (2020).
19. Fuss, S. et al. Negative emissions—Part 2: costs, potentials and side effects. *Environ. Res. Lett.* **13**, 063002 (2018).
20. Matthews, H. D. et al. Temporary nature-based carbon removal can lower peak warming in a well-below 2 °C scenario. *Commun. Earth Environ.* **3**, 65 (2022).
21. Jones, C. D. et al. Simulating the Earth system response to negative emissions. *Environ. Res. Lett.* **11**, 095012 (2016).
22. Rickels, W., Merk, C., Reith, F., Keller, D. P. & Oschlies, A. Misconceptions about modeling of negative emissions technologies. *Environ. Res. Lett.* **14**, 104004 (2019).
23. Smith, S. M. A case for transparent net-zero carbon targets. *Commun. Earth Environ.* **2**, 24 (2021).
24. Campbell-Arvai, V., Hart, P. S., Raimi, K. T. & Wolske, K. S. The influence of learning about carbon dioxide removal (CDR) on support for mitigation policies. *Clim. Change* **143**, 321–336 (2017).
25. Terlouw, T., Bauer, C., Rosa, L. & Mazzotti, M. Life cycle assessment of carbon dioxide removal technologies: a critical review. *Energy Environ. Sci.* **14**, 1701–1721 (2021).
26. Fuhrman, J., McJeon, H., Doney, S. C., Shobe, W. & Clarens, A. F. From Zero to Hero?: Why integrated assessment modeling of negative emissions technologies is hard and how we can do better. *Front. Clim.* **1**, 11 (2019).
27. Krause, A. et al. Large uncertainty in carbon uptake potential of land-based climate-change mitigation efforts. *Glob. Change Biol.* **24**, 3025–3038 (2018).
28. Melnikova, I. et al. Carbon cycle response to temperature overshoot beyond 2 °C – an analysis of CMIP6 models. *Earth's Future* **9**, e2020EF001967 (2021).
29. Harper, A. B. et al. Land-use emissions play a critical role in land-based mitigation for Paris climate targets. *Nat. Commun.* **9**, 2938 (2018).
30. Boysen, L. R. et al. Global climate response to idealized deforestation in CMIP6 models. *Biogeosciences* **17**, 5615–5638 (2020).
31. Bright, R. M. et al. Local temperature response to land cover and management change driven by non-radiative processes. *Nat. Clim. Change* **7**, 296–302 (2017).
32. Wang, J. et al. Global cooling induced by biophysical effects of bioenergy crop cultivation. *Nat. Commun.* **12**, 7255 (2021).
33. Cao, L., Bala, G., Caldeira, K., Nemani, R. & Ban-Weiss, G. Importance of carbon dioxide physiological forcing to future climate change. *Proc. Natl Acad. Sci. USA* **107**, 9513–9518 (2010).
34. Findell, K. L. et al. The impact of anthropogenic land use and land cover change on regional climate extremes. *Nat. Commun.* **8**, 989 (2017).
35. Gasser, T. & Ciais, P. A theoretical framework for the net land-to-atmosphere CO<sub>2</sub> flux and its implications in the definition of ‘emissions from land-use change’. *Earth Syst. Dyn.* **4**, 171–186 (2013).
36. Bauman, D. et al. Tropical tree mortality has increased with rising atmospheric water stress. *Nature* **608**, 528–533 (2022).
37. Dow, C. et al. Warm springs alter timing but not total growth of temperate deciduous trees. *Nature* **608**, 552–557 (2022).
38. Mitchard, E. T. A. The tropical forest carbon cycle and climate change. *Nature* **559**, 527–534 (2018).
39. Leng, G. & Hall, J. Crop yield sensitivity of global major agricultural countries to droughts and the projected changes in the future. *Sci. Total Environ.* **654**, 811–821 (2019).
40. Yue, C., Ciais, P., Houghton, R. A. & Nassikas, A. A. Contribution of land use to the interannual variability of the land carbon cycle. *Nat. Commun.* **11**, 3170 (2020).
41. Stenzel, F. et al. Irrigation of biomass plantations may globally increase water stress more than climate change. *Nature Communications* **12**, 1512 (2021).
42. Gvein, M. H. et al. Potential of land-based climate change mitigation strategies on abandoned cropland. *Commun. Earth Environ.* **4**, 39 (2023).
43. Churkina, G. et al. Buildings as a global carbon sink. *Nat. Sustain.* **3**, 269–276 (2020).
44. Mishra, A. et al. Land use change and carbon emissions of a transformation to timber cities. *Nat. Commun.* **13**, 4889 (2022).
45. Weng, Y., Cai, W. & Wang, C. Evaluating the use of BECCS and afforestation under China’s carbon-neutral target for 2060. *Appl. Energy* **299**, 117263 (2021).
46. O’Neill, B. C. et al. The Scenario Model Intercomparison Project (ScenarioMIP) for CMIP6. *Geoscientific Model Development* <https://doi.org/10.5194/gmd-9-3461-2016> (2016).
47. Boucher, O. et al. Presentation and evaluation of the IPSL-CM6A-LR climate model. *J. Adv. Modeling Earth Syst.* **12**, e2019MS002010 (2020).
48. Hurtt, G. C. et al. Harmonization of global land-use change and management for the Period 850–2100 (LUH2) for CMIP6. *Geosci. Model Dev. Discussions* **1**–65 <https://doi.org/10.5194/gmd-2019-360> (2020).
49. Friedlingstein, P. et al. Global carbon budget 2021. *Earth System Sci. Data Discussions* **2021**, 1–191 (2021).
50. Bondeau, A. et al. Modelling the role of agriculture for the 20th century global terrestrial carbon balance. *Glob. Change Biol.* **13**, 679–706 (2007).
51. Klein, D. et al. The value of bioenergy in low stabilization scenarios: an assessment using REMIND-MagPIE. *Climatic Change* **123**, 705–718 (2014).
52. IIASA. SSP Database (Shared Socioeconomic Pathways) – Version 2.0. <https://tntcat.iiasa.ac.at/SspDb/dsd?Action=htmlpage&page=welcome> (2018).
53. Gütschow, J., Jeffery, M. L., Günther, A. & Meinshausen, M. Country-resolved combined emission and socio-economic pathways based on the Representative Concentration Pathway (RCP) and Shared Socio-Economic Pathway (SSP) scenarios. *Earth System Science Data* **13**, 1005–1040 (2021).
54. Erb, K.-H., Haberl, H. & Plutzar, C. Dependency of global primary bioenergy crop potentials in 2050 on food systems, yields, biodiversity conservation and political stability. *Energy Policy* **47**, 260–269 (2012).
55. Ai, Z., Hanasaki, N., Heck, V., Hasegawa, T. & Fujimori, S. Simulating second-generation herbaceous bioenergy crop yield using the global hydrological model H08 (v.bio1). *Geosci. Model Dev.* **13**, 6077–6092 (2020).
56. Li, W., Ciais, P., Makowski, D. & Peng, S. A global yield dataset for major lignocellulosic bioenergy crops based on field measurements. *Sci. Data* **5**, 180169 (2018).
57. Jones, C. D. et al. C4MIP: the coupled climate–carbon cycle model intercomparison project: experimental protocol for CMIP6. *Geosci. Model Dev.* **9**, 2853–2880 (2016).
58. WCRP. World Climate Research Programme (WCRP) Coupled Model Intercomparison Project (Phase 6). <https://esgf-node.llnl.gov/search/cmip6/> (2022).
59. UoM. Land-Use Harmonization (LUH2) of University of Maryland, Global Ecology Laboratory. <https://luh.umd.edu/data.shtml> (2022).
60. Schulzweida, U. CDO User Guide. <https://doi.org/10.5281/zenodo.7112925> (2022).

## Acknowledgements

The IPSL-CM6 simulations were performed using the HPC resources of TGCC under the allocation 2021-A0100107732 (project gencmip6) provided by GENCI (Grand Equipement National de Calcul Intensif). This work benefited from the technical support and discussions with several researchers: Daniel Goll and Sébastien Nguyen at LSCE (France), Matteo Mastroianni at Ca’Foscari University (Italy), Jörg Schwinger at Bjerknes Centre for Climate Research (Norway), Nico Bauer at Potsdam Institute for Climate Impact Research (Germany) and Tokuta Yokohata at NIES (Japan). This work benefited from State assistance managed by the National Research Agency in France under the Programme d’Investissements d’Avenir under the reference ANR-19-MPGA-0008. This project has received funding from the European Union’s Horizon 2020 research and innovation programme under Grant Agreement No. 101003536 (ESM2025 – Earth System Models for the Future). We further acknowledge the Program for the Advanced Studies of Climate Change Projection (SENTAN, grant number JPMXD0722681344) from the Ministry of Education, Culture, Sports, Science and Technology (MEXT), Japan.



### Author contributions

I.M. performed IPSL-CM6A-LR simulations, data analysis and wrote the initial draft. O.B. and P.C. initiated the study. O.B., P.C., K.T., and N.V. supervised the study. All authors provided input into developing the study ideas and contributed to writing the manuscript

### Competing interests

The authors declare no competing interests.

### Additional information

**Supplementary information** The online version contains supplementary material available at <https://doi.org/10.1038/s43247-023-00866-7>.

**Correspondence** and requests for materials should be addressed to Irina Melnikova.

**Peer review information** *Communications Earth & Environment* thanks Michael Gregory Windisch, John Field and the other, anonymous, reviewer(s) for their contribution to the peer review of this work. Primary Handling Editor: Aliénor Lavergne. A peer review file is available.

**Reprints and permission information** is available at <http://www.nature.com/reprints>

**Publisher's note** Springer Nature remains neutral with regard to jurisdictional claims in published maps and institutional affiliations.



**Open Access** This article is licensed under a Creative Commons Attribution 4.0 International License, which permits use, sharing, adaptation, distribution and reproduction in any medium or format, as long as you give appropriate credit to the original author(s) and the source, provide a link to the Creative Commons license, and indicate if changes were made. The images or other third party material in this article are included in the article's Creative Commons license, unless indicated otherwise in a credit line to the material. If material is not included in the article's Creative Commons license and your intended use is not permitted by statutory regulation or exceeds the permitted use, you will need to obtain permission directly from the copyright holder. To view a copy of this license, visit <http://creativecommons.org/licenses/by/4.0/>.

© The Author(s) 2023